Available online at www.sciencedirect.com
ScienceDirect
Differential Geometry and its Applications 26 (2008) 140–150
DIFFERENTIAL GEOMETRY AND ITS APPLICATIONS
www.elsevier.com/locate/difgeo

Fractional monodromy: parallel transport of homology cycles

Andrea Giacobbe

Università di Padova, Dipartimento di Matematica Pura e Applicata, Via Trieste 63, 35131 Padova, Italy

Received 6 October 2005; received in revised form 14 October 2006

Available online 31 December 2007

Communicated by P. Michor

Abstract

A $2n$-dimensional completely integrable system gives rise to a singular fibration whose generic fiber is the n-torus T^n. In the classical setting, it is possible to define a parallel transport of elements of the fundamental group of a fiber along a path, when the path describes a loop around a singular fiber, it defines an automorphism of $\pi_1(T^n)$ called monodromy transformation [J.J. Duistermaat, On global action-angle coordinates, Communications on Pure and Applied Mathematics 33 (6) (1980) 687–706]. Some systems give rise to a non-classical setting, in which the path can wind around a singular fiber only by crossing a codimension 1 submanifold of special singular fibers (a wall), in this case a non-classical parallel transport can be defined on a subgroup of the fundamental group. This gives rise to what is known as monodromy with fractional coefficients [N. Nekhoroshev, D. Sadovskiĭ, B. Zhilinskiĭ, Fractional monodromy of resonant classical and quantum oscillators, Comptes Rendus Mathematique 335 (11) (2002) 985–988]. In this article, we give a precise meaning to the non-classical parallel transport. In particular we show that it is a homologic process and not a homotopic one. We justify this statement by describing the type of singular fibers that generate a wall that can be crossed, by describing the parallel transport in a semi-local neighbourhood of the wall of singularities, and by producing a family of 4-dimensional examples.

MSC: 55R55; 37J35

Keywords: Torus bundle with singularities; Momentum map; Fractional monodromy; Parallel transport; Homology and homotopy

1. Introduction

1.1. Notations

A completely integrable system is a $2n$-dimensional symplectic manifold M endowed with n Poisson-commuting functions $F_1, \ldots, F_n$ such that $F = (F_1, \ldots, F_n) : M \to \mathbb{R}^n$ has compact level sets. The map F is called *momentum map*, its image is called *momentum domain* $\mathcal{M}$ and the set of F-regular values is called *regular momentum domain* $\mathcal{M}_{\text{reg}}$. The F-preimage $\Lambda_{f_1,\ldots,f_n} = F^{-1}(f_1, \ldots, f_n)$ of any regular value $(f_1, \ldots, f_n)$ is isomorphic to a set of finitely many disjoint tori and is called *regular fiber*. It follows that, omitting to consider the inessential complication of multiply connected preimages (see [16]), the map $F : M_{\text{reg}} = F^{-1}(\mathcal{M}_{\text{reg}}) \to \mathcal{M}_{\text{reg}}$ is a torus bundle. On the other

E-mail address: giacobbe@math.unipd.it.

0926-2245/$ – see front matter
doi:10.1016/j.difgeo.2007.11.011

Fig. 1. Typical momentum domain and bifurcation diagram for 4-dimensional systems appearing in connection to classical integral monodromy (left) and to non-classical fractional monodromy (right).

hand, the momentum map defines a fibration whose fibers above non-regular values are not necessarily tori and are called *singular fibers*.

The Liouville–Arnol'd theorem states that around any regular fiber of a given completely integrable system, one can always find a set of semi-local action-angle coordinates. In [6], Duistermaat describes the obstructions to global existence of action-angle coordinates. One of these obstructions is the *monodromy* of the torus bundle $F : M_{\text{reg}} \to \mathcal{M}_{\text{reg}}$.

1.2. Classical parallel transport and monodromy

The spherical pendulum [6] was the first (4-dimensional) example of a completely integrable system with non-trivial monodromy. Its momentum domain $\mathcal{M}$ has an isolated singularity (see Fig. 1 left). Using Cushman's argument to compute the monodromy of the system, one chooses basic cycles a, b of the fundamental group of a generic fiber T^2, deforms them fiberwise continuously around the isolated singularity, and proves that the cycle a deforms into the cycle $a + b$ while the cycle b deforms into itself. The conclusion is that the 2-torus bundle has non-trivial monodromy.

After this first example, non-trivial monodromy appeared in many physical systems, and has been shown to play a role both in classical [2,7,15] as well as in quantum systems [3,4,9,10,14]. All such examples share the property of having a non-simply connected regular momentum domain where monodromy can be computed classically and is a representation of the group $\pi_1(\mathcal{M}_{\text{reg}}, (\bar{f}_1, \ldots, \bar{f}_n))$ into $\text{GL}(\pi_1(\Lambda_{\bar{f}_1,\ldots,\bar{f}_n})) \simeq \text{SL}(n, \mathbb{Z})$.

In many cases the fundamental group $\pi_1(\mathcal{M}_{\text{reg}}, (\bar{f}_1, \ldots, \bar{f}_n))$ is isomorphic to $\mathbb{Z}$, the monodromy representation is hence uniquely determined by the image in $\text{SL}(n, \mathbb{Z})$ of a generator of $\pi_1(\mathcal{M}_{\text{reg}}, (\bar{f}_1, \ldots, \bar{f}_n))$. For this reason in the literature one often refers to the *monodromy matrix* associated to a completely integrable system. We will abuse notations precisely in this sense.

A monodromy matrix can be computed as follows: choose a basis of cycles a_i (the *initial basis*) of the fundamental group $\pi_1(\Lambda_{\bar{f}_1,\ldots,\bar{f}_n}) = \{\prod_j a_j^{n_j} \mid n_j \in \mathbb{Z}\} \simeq \mathbb{Z}^n$ of a given regular fiber (the *base fiber*), transport the cycles a_i *fiberwise continuously* from torus to torus along a loop γ in $\mathcal{M}_{\text{reg}}$. Once back to the base fiber consider the cycles thus obtained. The transport of the cycles a_i has deformed them into cycles $b_i = \prod_j a_j^{n_{ij}}$ (the *final basis*). The matrix (n_{ij}) is an element of $\text{SL}(n, \mathbb{Z})$ and is called the *monodromy matrix* associated to the loop γ written with respect to the basis a_i. Observe that this can always be done, in a non-unique way, because of the local triviality of the bundle.

Naturally, there are many possible *fiberwise continuous deformations* of a cycle along a path γ in $\mathcal{M}_{\text{reg}}$. Each deformation is the immersion of a cylinder in M_{reg} that projects onto γ. Different fiberwise continuous deformations yield final cycles that are homotopic. It follows that the process of fiberwise continuous deformation defines a transport among fundamental groups of regular fibers. This justifies the word *parallel transport of cycles*. Moreover, the transport depends only on the homotopy class with fixed endpoints of the path γ within $\mathcal{M}_{\text{reg}}$ (which amounts to local flatness).

In describing the parallel transport we have ignored one relevant fact: the choice of a base point of the cycles a_i. It is a known fact that the first homology group is the quotient of the fundamental group by its commutator subgroup (the Abelianization of the fundamental group), and that the set of loops up to homotopy without the specification of a base point is the set of conjugacy classes in the fundamental group [5] (not a group, but a set that submerges the Abelianization of the fundamental group).

The choice of a base point is immaterial when the topological space under investigation has commutative fundamental group, in fact in that case the fundamental group, the first homology group and the conjugacy classes of the fundamental group are all the same set. But the base point becomes essential when the fundamental group is non-commutative. Forgetting it, has the effect of erasing the order of multiplication of cycles. We will show that com-

muting two cycles is precisely what is needed to parallel transport through a wall of singular values in a system with fractional monodromy, and is precisely what makes the non-classical parallel transport a homologic process.

1.3. Non-classical parallel transport: cobordism through corank 1 hyperbolic singularities

The regular fibers of a completely integrable system are n-tori, their fundamental group is commutative, and they give rise to a torus bundle that allows the definition of parallel transport. These facts become false in the presence of singular fibers. The existence of momentum domains with a line of singular values as in Fig. 1 right and the analysis of quantum spectra around such line, convinced B. Zhilinskiĭ of the existence of a fractional monodromy associated to the parallel transport of cycles along the path in the figure. To compute such monodromy one needs to extend the definition of parallel transport to these singular cases. The practical question becomes: is it possible to parallel transport the basis cycles a_i described above along a path γ that crosses a set of singular values as that depicted in Fig. 1 right? Much efforts have been taken to answer this question [8,11,12]. This work is part of such efforts, and its original contribution rests in the description of the local geometry of the walls of singular fibers through which it is possible to extend the definition of parallel transport, and the observation that the objects to be parallel transported are homology cycles.

More precisely, in Section 2 we define the type of singular values that a path γ is allowed to cross, we show that the singular fibers above such singular values have non-commutative fundamental group, and we extend the definition of parallel transport along paths that cross such values proving two facts:

1. that the parallel transport is defined on an index 2 subgroup of the fundamental group,
2. that it is well defined of homology cycles.

The first fact justifies the name *fractional monodromy*: assume to be given a transformation of $\mathbb{Z}^2$ to itself that, with respect to the canonical basis $\{e_1, e_2\}$, is represented by the matrix $\left(\begin{smallmatrix}1 & 0\\ 1 & 1\end{smallmatrix}\right)$. Then the transformation on the subgroup $\mathbb{Z}\{2e_1, e_2\}$, written with respect to the basis $\{2e_1, e_2\}$, is represented by the matrix $\left(\begin{smallmatrix}1 & 0\\ 2 & 1\end{smallmatrix}\right)$. So, if a transformation can be defined on the subgroup $\mathbb{Z}\{2e_1, e_2\}$ and is given by the matrix $\left(\begin{smallmatrix}1 & 0\\ 1 & 1\end{smallmatrix}\right)$, then the corresponding transformation of $\mathbb{Z}^2$ with respect to the canonical basis $\{e_1, e_2\}$ must be represented by the matrix $\left(\begin{smallmatrix}1 & 0\\ 1/2 & 1\end{smallmatrix}\right)$.

The second fact can be otherwise stated by saying that the extension of parallel transport through singular fibers does not correspond to the fiberwise immersion of a cylinder but rather to a fiberwise cobordism, that is the immersion of a 2-dimensional manifold whose boundary are the initial and final cycle.

In Section 3 we describe a local model that justifies the appearance of bigger denominators in the monodromy matrix. In Sections 4 and 5 we present 4-dimensional completely integrable systems in which fractional monodromy can be computed and is defined in $\mathbb{Z}_{(2)}$, respectively $\mathbb{Z}_{(q)}$, where $\mathbb{Z}_{(q)}$ is the ring of fractions with denominator a power of q.

2. Local model for $\frac{1}{2}$ fractional monodromy

Let us begin by describing the type of singularities that give origin to fractional monodromy.

Singularities of hyperbolic type have been analyzed by Bolsinov, Matveev and Fomenko in what we call the BMF-classification [1]. This classification deals with corank 1 singularities for 4-dimensional Hamiltonian systems and it has been extended by Zung [16] to any dimension. Let us briefly recall the results in these two works.

Given a completely integrable system (M, F), the corank of a singular point x in M is the natural number $n - \operatorname{rank} d_x F$. At a corank k singular point there are k functions H_j, linear combinations of the F_i, such that $d_x H_j = 0$. The Hessian of the functions H_j define a commutative subalgebra in the Lie algebra of quadratic polynomials of any maximal symplectic subspace of $\ker d_x F$, that is any algebraic complement in $\ker d_x F$ to the $(n-k)$-dimensional space generated by the vectors X_{F_i}. A singular point of corank k is said to be a *non-degenerate* singularity if the commutative subalgebra $\mathbb{R}\{\operatorname{Hess} H_j\}$ has dimension k and is hence a Cartan subalgebra.

As was shown in [16], a saturated neighbourhood of a singular fiber containing corank 1 hyperbolic type singular points is isomorphic to $\mathbb{R}^{n-1}_I \times T^{n-1}_\alpha \times P$ or is doubly-covered by such space. The manifold P is one of the 2-dimensional manifolds with boundary described in the BMF-classification and there called *letter-atoms*.

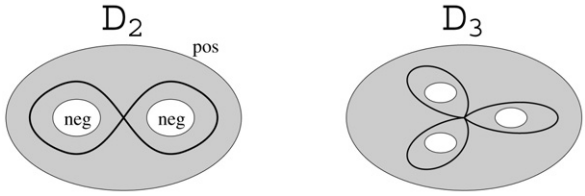

Fig. 2. Basis of Seifert fibrations obtained fixing $I = \text{const}$. D_2 is also a letter-atom for the representation ∞. Observe the labelling of the boundary circles as positive or negative and the figure eight critical level-set.

The manifold P is the thickening of a graph Γ, its boundary is the disjoint union of circles (in Fig. 2 left is the thickening of the graph with one vertex and two edges). Some of the circles in the boundary of the thickening are called *positive*, the others are called *negative*, according to the rule that each edge of the graph that touches a positive circle on one side must touch a negative circle on the other side (rule (3) in page 68 of [1]). The momentum map is the map $(I_1, \ldots, I_{n-1}, J)$ from $\mathbb{R}^{n-1}_I \times T^{n-1}_\alpha \times P$ to $\mathbb{R}^n$, where J is a map from P to $\mathbb{R}$ whose level sets are the concentric circles outlining the graph Γ in its thickening. J monotonically increases moving towards the positive circles and monotonically decreases moving towards the negative circles. The critical level of J is the graph Γ, which is assumed to be at $J = 0$. The critical points of J are the vertices of the graph Γ, each vertex has 4 departing edges.

From this local description it immediately follows that the momentum domain is the n-dimensional ball divided in two connected components by a codimension 1 surface of singularities (its equatorial $n-1$ ball, given by the equation $J = 0$). The fibers at $J = 0$ contain non-degenerate corank 1 hyperbolic-type singular points, the regular levels are the direct product of the T^{n-1}_α with the concentric circles in P.

Fact 1. *All the cycles parameterized by the variables α can be transported with the classical smooth parallel transport from the fibers sitting above points in which J is positive to fibers sitting above points in which J is negative. On the other hand, the cycle represented by the union of positive circles in P is cobordant to the cycle represented by the union of negative circles. The cobordism between the cycles is the manifold P itself.*

Remark. If the neighbourhood of the singular fiber is doubly covered by the space $\mathbb{R}^{n-1}_I \times T^{n-1}_\alpha \times P$, the cobordism is obtained by projecting P.

Remark. When the neighbourhood of the singular fiber is doubly covered by the space $\mathbb{R}^{n-1}_I \times T^{n-1}_\alpha \times P$, the number of components of the fiber does not change across the singular line.

Let us clarify these statements with the simplest yet fundamental example.

Example. This example is the local model for the codimension 1 hyperbolic singularity that, in the BMF-classification, corresponds to the representation $\circlearrowright$. This is the first system of the list in [1] whose regular level-sets are connected 2-tori.

The phase space of this example is $\mathbb{R}_I \times E_2$, where E_2 is a Seifert circle bundle with a singular circle of weight 2. The bundle E_2 is a cylinder $D_2 \times [0, 2\pi]$ whose upper side $D_2 \times \{2\pi\}$ is identified with the lower side $D_2 \times \{0\}$ after a rotation of π, here the base D_2 is drawn in Fig. 2 left. The vertical lines of the cylinder, taken in couples, form circles. The center-line is a circle of half-length.

On the space D_2 is defined a real-valued function J that can be extended to E_2. By convention, the critical level is posed at $J = 0$ and is the figure eight drawn in black in Fig. 2 left. The levels with J positive are two circles inside the figure eight while the levels with J negative are circles surrounding it.

The momentum map of this system is the function $(I, J) : \mathbb{R}_I \times E_2 \to \mathbb{R}^2$ and its image is a disk divided into two connected components (the J-positive half-disk and the J-negative half-disk) by a codimension 1 surface of singularities whose fibers contain corank 1 hyperbolic-type singular points. The regular fibers are connected 2-tori, while the singular fibers are obtained by twisting and gluing the extremes of a cylinder on the figure eight drawn in black in Fig. 2 left, and are 2-*curled tori* C_2.

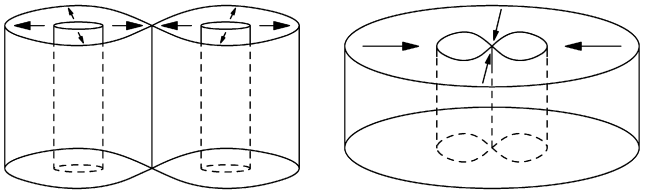

Fig. 3. The gradient flow of J allows the definition of maps σ from T^+ to C_2 (left) and ι from T^- to C_2 (right).

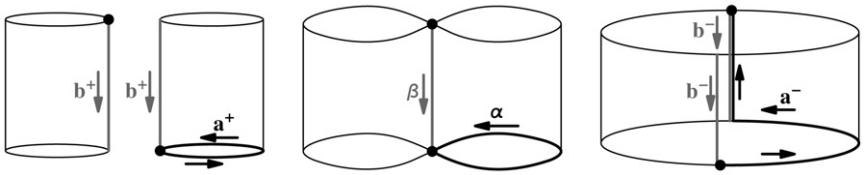

Fig. 4. A basis of cycles of the fundamental group for regular fibers T^+ (left) and T^- (right) and for singular fibers C_2. The thick dot is the base point.

Fact 2. *This local model already exposes the fact that the parallel transport is a homologic, and not a homotopic process.*

First, observe that the fundamental group of the curled torus C_2 is non-commutative, it is in fact generated by two elements α, β with the relation $\alpha\beta^2 = \beta^2\alpha$. Second, the levels in E_2 with positive J can be guided (with normalized-gradient flow of J) to the critical fiber C_2, same for the levels with negative J, see Fig. 3. This defines two continuous maps, $\sigma : T^+ \to C_2$ and $\iota : T^- \to C_2$, where T^+ is a level set with $J > 0$, $I = \text{const}$ and T^- is a level set with $J < 0$, $I = \text{const}$.

The parallel transport of homotopy cycles can hence be defined on both sides of the singular value of J *up to the critical level set* and gives rise to two images

$$\Sigma = \sigma^*\big(\pi_1(T^+, \bullet)\big), \qquad \mathcal{I} = \iota^*\big(\pi_1(T^-, \bullet)\big)$$

of the fundamental group of a 2-torus into $\pi_1(C_2, \bullet)$, where $\bullet$ is the base point.

Denoting by a^+, b^+ a basis of cycles for the tori T^+, by a^-, b^- a basis of cycles for the tori T^-, and by α, β a basis of cycles for the curled torus C_2 as in Fig. 4, one can easily see that a^+ maps to α, b^+ to β^2, a^- to $\alpha\beta^{-1}$ and b^- to β^2.

Definition 1. We say that an element of the first homotopy (or first homology) of a regular fiber is *passable* through a codimension one singularity if its image on the singular fiber is also image of a cycle of regular fibers on the other side of the singularity. A subgroup is passable if all its elements are passable.

It follows that both Σ and $\mathcal{I}$ are index two subgroups of $\pi_1(C_2, \bullet)$. But the elements of Σ are all of the form $\alpha^n\beta^{2m}$, while those in $\mathcal{I}$ are of the form $(\alpha\beta^{-1})^n\beta^{2m}$. The intersection of the two subgroups is a group isomorphic to $\mathbb{Z}$, and contains all and only elements of the form β^{2m}.

Homotopically, the only passable subgroup of $\pi_1(T^+, \bullet)$ is that generated by the element b^+, which maps in β^2 and can be continued in $\pi_1(T^-, \bullet)$ as b^-. The scenario completely changes using homology. The main difference is that a curled torus is a homology-torus. The two homotopy cycles α, β project to homology cycles $[\alpha], [\beta]$ that commute.

Denoting by $[a^+]$, $[b^+]$ a basis for the first homology group of the tori T^+, and by $[a^-]$, $[b^-]$ a basis for the first homology group of the tori T^-, one obtains that $[a^+]$ maps to $[\alpha]$, $[b^+]$ to $2[\beta]$, $[a^-]$ to $[\alpha] - [\beta]$ and $[b^-]$ to $2[\beta]$. Hence, the index two subgroup of $H_1(T^+, \mathbb{Z})$ generated by $2[a^+]$, $[b^+]$ maps onto the index 4 subgroup of $H_1(C_2, \mathbb{Z})$ generated by $2[\alpha]$, $2[\beta]$. But also the index two subgroup of $H_1(T^-, \mathbb{Z})$ generated by $2[a^-]$, $[b^-]$ maps onto the same index 4 subgroup.

It follows that the parallel transport can be defined onto the index 2 subgroup of $H_1(T^+, \mathbb{Z})$ generated by $2[a^+], [b^+]$. These two cycles map respectively to $2[\alpha], 2[\beta]$ and can be continued in $H_1(T^-, \mathbb{Z})$ as $2[a^-] + [b^-], [b^-]$. To compute monodromy one should continue the parallel transport along a path that completes the loop around an essential singularity and back to T^+. This cannot be done in a semi-local model but will be performed in the 4-dimensional systems in Sections 4 and 5.

3. Local models for bigger denominators

The example above indicates the appearance of a 2 in the denominators of the monodromy matrix. Bigger denominators cannot arise in completely integrable systems possessing non-degenerate hyperbolic singularities. Without pretense of giving a classification, we provide in this subsection a semi-local model that explains the appearance of a monodromy matrix with coefficients in $\mathbb{Z}_{(q)}$. In this model the singularities are degenerate in the Morse–Bott sense, and are a semi-local model for the singularities of the family of completely integrable systems that we present in Section 5.

Example. The phase space of this example is the space $\mathbb{R}_I \times E_q$, where E_q is a Seifert circle bundle with a singular circle of length $1/q$. The bundle E_q can be obtained from the cylinder $D_q \times [0, 2\pi]$ identifying the upper side $D_q \times \{2\pi\}$ of the cylinder with its lower side $D_q \times \{0\}$ after a rotation of $2\pi/q$, here D_q is the domain in Fig. 2 right (drawn for $q = 3$). The vertical lines of the cylinder, taken in q-ples, form a circle. The center-line is a circle of length $1/q$.

On the space D_q is defined a function J that can be extended to E_q. The levels $J = c$ in E_q are the trefoil with q petals (a q-foil) when $c = 0$ (drawn in black for $q = 3$ in Fig. 2 right), are q concentric circles inside the q-foil if $c > 0$, are a big circle surrounding the q-foil when $c < 0$. The momentum map is the function $(I, J) : \mathbb{R}_I \times E_q \to \mathbb{R}^2$. The image of the momentum map is a disk divided into two connected components by a codimension 1 surface of singularities whose fibers contain corank 1 degenerate singularities. The regular fibers are connected 2-tori, while the singular fibers are *q-curled tori* C_q.

A q-curled torus has fundamental group that is a group on two generators α, β with the relation $\alpha\beta^q = \beta^q\alpha$ (see Fig. 5). Also in this case, the gradient descent of J in $E_q = \{I = \text{const}\}$ defines two continuous maps, $\sigma : T^+ \to C_q$ and $\iota : T^- \to C_q$. It is possible to perform a parallel transport of homotopy cycles on both sides of the singular value of J up to the critical level set and obtain the images

$$\Sigma = \sigma^*\big(\pi_1(T^+, \bullet)\big), \qquad \mathcal{I} = \iota^*\big(\pi_1(T^-, \bullet)\big).$$

With an appropriate choice of a basis $\{a^+, b^+\}$ of the fundamental group of the tori T^+, a basis $\{a^-, b^-\}$ of the fundamental group of the tori T^-, and a basis $\{\alpha, \beta\}$ of the fundamental group of the curled torus C_q, we have that a^+ maps to α, b^+ to β^q, a^- to $\alpha\beta^{-1}$ and b^- to β^q. The two subgroups Σ and $\mathcal{I}$ are index q subgroups of $\pi_1(C_q, \bullet)$, their intersection is isomorphic to $\mathbb{Z}$ and consists of elements of the form β^{qm}.

Also in this case $[\alpha]$ and $[\beta]$ form a basis for the first homology of the singular fibers C_q, that are homology-tori. Denoting by $[a^+], [b^+]$ a basis for the first homology of the tori T^+, and by $[a^-], [b^-]$ a basis for the first homology of the tori T^-, one obtains that $[a^+]$ maps to $[\alpha]$, $[b^+]$ to $q[\beta]$, $[a^-]$ to $[\alpha] - [\beta]$ and $[b^-]$ to $q[\beta]$. Hence, the index q subgroup generated by $q[a^+], [b^+]$ maps onto the index q^2 subgroup of $H_1(C_q, \mathbb{Z})$ generated by $q[\alpha], q[\beta]$. Also the index q subgroup of $H_1(T^-, \mathbb{Z})$ generated by $q[a^-], [b^-]$ maps onto the same index q^2 subgroup. It follows that

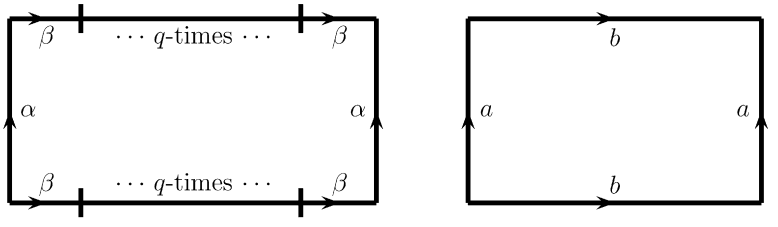

Fig. 5. The cut-and-paste representation of a q-curled torus and of a regular 2-dimensional torus.

the parallel transport can be defined on the index q subgroup of $H_1(T^+, \mathbb{Z})$ generated by $q[a^+], [b^+]$. These cycles map respectively to $q[\alpha], q[\beta]$ and can be continued as $q[a^-] + [b^-], [b^-]$ in $H_1(T^-, \mathbb{Z})$.

4. An example with monodromy in SL(2, $\mathbb{Z}_{(2)}$)

In this section we present a 4-dimensional system whose singularities are precisely as those described in the semi-local model of Section 2. This example, as well as those presented in Section 5, are the model systems that were used to prove the existence of fractional monodromy [8,11,12]. Consider the completely integrable system in which the phase space is $\mathbb{C}_z \times \mathbb{C}_w$ and the two commuting functions are

$$J = \frac{1}{2}|z|^2 - |w|^2, \quad H = \sqrt{2}\,\Im(z^2 w) + 2\,|z|^2|w|^2.$$

The Hamiltonian flow of J is the circle action of the $1 : -2$ harmonic oscillator.

4.1. The fibration defined by the momentum map

The two functions J, H define a momentum map $(J, H) : \mathbb{C}^2 \to \mathbb{R}^2$ that has compact and connected level sets. The image of the momentum map is depicted in Fig. 6 left (on the right is shown a neighbourhood of the origin). The critical values of the momentum map are of three types: the origin, whose fiber is a *pinched torus*, the set $(-\frac{1}{2}, 0) \times \{0\}$, whose fibers are 2-*curled tori*, and the points in the boundary of the momentum domain, uninteresting to us, whose fibers are circles.

One way to prove these facts is to analytically describe the level sets $\Lambda_{j,h} = \{(z, w) | J(z, w) = j, H(z, w) = h\}$. Assume at first that j is negative. The condition $J = j$ implies that $|w|^2 = -j + \frac{1}{2}|z|^2$. It follows that the norm of w is always bigger than $-j > 0$. Hence, the level set $J = j$ is isomorphic to the manifold $\mathbb{C}_z \times S^1_\vartheta$, its embedding in the phase space $\mathbb{C}^2$ is given by

$$\mathbb{C}_z \times S^1_\vartheta \to \mathbb{C}_z \times \mathbb{C}_w \quad (z, \vartheta) \mapsto \left(z, e^{i\vartheta}\frac{\sqrt{2}}{2}\sqrt{|z|^2 - 2j}\right).$$

In the manifold $\mathbb{C}_z \times S^1_\vartheta$ the levels sets $H = h$ are given by the equation

$$\sqrt{|z|^2 - 2j}\,\Im(z^2 e^{i\vartheta}) + |z|^2\big(|z|^2 - 2j\big) = h.$$

Assume now that j is positive, the condition $J = j$ implies that $|z|^2 = 2j + 2|w|^2$. It follows that the norm of z is always bigger than $2j > 0$. Hence, the level set $J = j$ is isomorphic to the manifold $\mathbb{C}_w \times S^1_\varphi$. Its embedding in the phase space $\mathbb{C}^2$ is given by

$$\mathbb{C}_w \times S^1_\varphi \to \mathbb{C}_z \times \mathbb{C}_w \quad (w, \varphi) \mapsto \big(e^{i\varphi}\sqrt{2}\sqrt{|w|^2 + j}, w\big).$$

In the manifold $\mathbb{C}_w \times S^1_\varphi$, the level sets $H = h$ are given by the equation

$$2\sqrt{2}\big(|w|^2 + j\big)\Im(e^{2i\varphi} w) + 4\big(|w|^2 + j\big)|w|^2 = h.$$

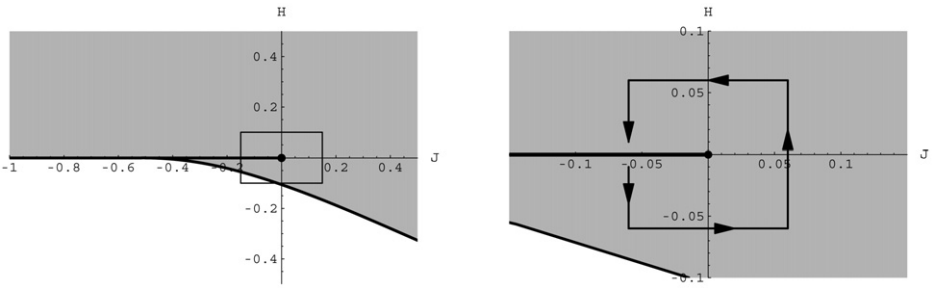

Fig. 6. The momentum domain on the left. On the right the loop we use to compute fractional monodromy

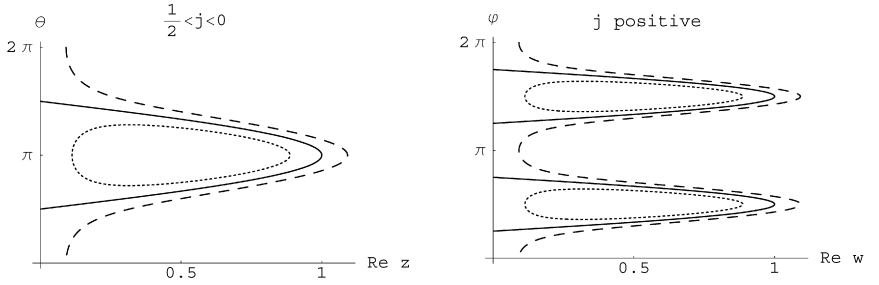

Fig. 7. Intersections between three level sets $\Lambda_{j,h}$ and half-planes. Dotted is the intersection with a level having negative h, continuous is the intersection with a level having $h = 0$, dashed is the intersection with a level having positive h.

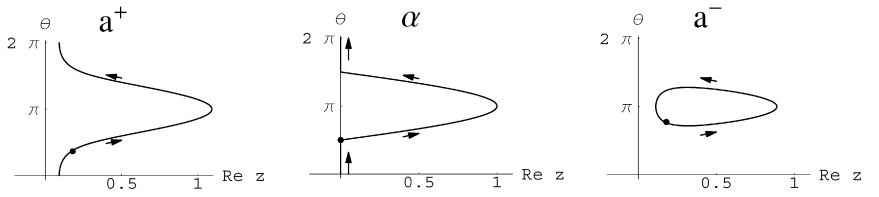

Fig. 8. The cycles $a^{\pm}$ and α. The thick dot is the base point.

The level sets of the above equations, that are the sets $\Lambda_{j,h}$, can be viewed as immersed hypersurfaces of $C_z \times S^1_{\vartheta}$ ($C_w \times S^1_{\varphi}$ respectively), and can hence be plotted in the covering $\mathbb{C}_z \times \mathbb{R}_{\tilde{\vartheta}}$ ($\mathbb{C}_w \times \mathbb{R}_{\tilde{\varphi}}$ respectively) as hypersurfaces which are 2π-periodic in the last variable. The best way to visualize such hypersurfaces is to picture the curve obtained by sectioning them with the half-plane $\Im z = 0, \Re z > 0$ ($\Im w = 0, \Re w > 0$ respectively). The result of this intersection is drawn in Fig. 7. In the j-negative case, the full level set is the manifold obtained by rotating that curve around the $\mathbb{R}_{\tilde{\vartheta}}$ axes and lowering it of twice the angle of rotation. In the j-positive case the full level-set is obtained by rotating the curve around the $\mathbb{R}_{\tilde{\varphi}}$ axes, but this time the curve must be lowered of half the angle of rotation. In Section 6 (Appendix) we explain how we obtained such description.

From this representation one can easily see that all the level sets are connected 2-tori except for the levels $\Lambda_{j,h}$ with $h \leqslant 0$. Let us analyze only the troublesome levels that touch the $\mathbb{R}_{\tilde{\vartheta}}$ axes ($\mathbb{R}_{\tilde{\varphi}}$ respectively) and whose graph looks non-smooth. When $-\frac{1}{2} < j < 0$ the level $\Lambda_{j,0}$ can be described with cut-and-paste topology: remove from $\Lambda_{j,0}$ the center-line $z = 0$, the complement is a cylinder open at both boundary circles. The ends of the cylinder must be glued along the circle $\{0\} \times S^1_{\vartheta}$ with a 2–1 map. The resulting topological space is a 2-curled torus.

The description changes when dealing with the case $j > 0$. In that case it is still true that the complement of the center-line $w = 0$ is a cylinder open at both ends, but the boundary has to be glued to the circle $\{0\} \times S^1_{\varphi}$ with a 1–1 map. The topological space is a torus.

4.2. *The definition and parallel transport of the cycles*

Consider now a loop γ that winds around the origin once, as in Fig. 6 right. Fixing $-\frac{1}{2} < j < 0$, the definition of a basis of cycles a^+, b^+ of the fundamental group of the fibers $\Lambda_{j,h}$ with $h > 0$, the definition of a basis a^-, b^- of the fundamental group of the fibers $\Lambda_{j,h}$ with $h < 0$, and the definition of a basis α, β of the fundamental group of the fibers $\Lambda_{j,0}$, can be done by pictures. In Fig. 8 we only plot the cycles a^+, α, a^-. The cycles b^+, β, b^- are orbits of the $1 : -2$ oscillator, hence are descending spirals winding around the $\tilde{\vartheta}$-axes.

The definition of the cycles shows, as expected, that a^+ maps to α, a^- maps to $\alpha\beta^{-1}$. Of course, $b^{\pm}$ both map to β^2.

Fixing now $j > 0$, one can similarly draw a basis of cycles c^+, d^+ of the fundamental group of the fibers $\Lambda_{j,h}$ with $h > 0$, c^-, d^- of the fundamental group of the fibers $\Lambda_{j,h}$ with $h > 0$, and χ, δ of the fundamental group of the fibers $\Lambda_{j,0}$. See Fig. 9.

In this case the images of the cycles $c^{\pm}$ and $d^{\pm}$ in $\pi_1(\Lambda_{j,0})$ is simpler to describe. In fact $c^{\pm}$ both map to χ and $d^{\pm}$ both map to δ.

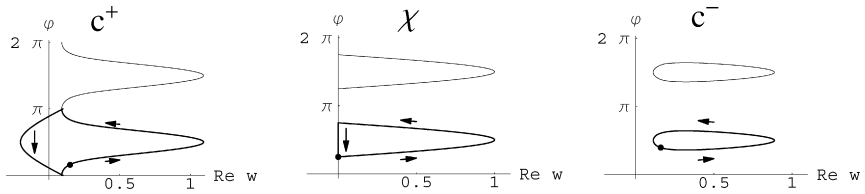

Fig. 9. The cycles $c^{\pm}$ and χ. The descending part of the path c^+ does not belong to the plane $\Re w \times \vartheta$ but winds around the φ-axes. The thick dot is the base point.

Parallel transporting the cycles a^+, b^+ along the part of γ at a fixed $h > 0$ from level sets with $j < 0$ to level sets with $j > 0$, and expressing the final cycles with respect to the basis c^+, d^+, one obtains that a^+ is homotopic to c^+ and b^+ is homotopic to d^+ (this second fact does not require a proof, since both b^+, d^+ are orbits of the J-action). The same process applied to the cycles a^-, b^- gives that a^- parallel transports to c^- and b^- to d^-.

4.3. The fractional monodromy map

We can now compute the monodromy matrix. We make use right from the beginning of homology cycles, since the homotopic process encounters the problems described in the Introduction.

When $j < 0$ and $h > 0$, the smoothly varying homology cycles $2[a^+]$ parallel transport up to the critical fiber $\Lambda_{j,0}$ to the cycles $2[\alpha]$, while the cycles $[b^+]$ transport to the cycles $2[\beta]$. Lifting the image from the other side, the cycle $2[\alpha]$ is the image of the cycles $2[a^-] + [b^-]$, while the cycle $2[\beta]$ is the image of $[b^-]$. So, the parallel transport deforms the cycles $2[a^+]$ into the cycles $2[a^-] + [b^-]$ and $[b^+]$ to $[b^-]$.

It follows that, continuing the parallel transport to the level-sets $\Lambda_{j,h}$ with $j > 0$ and $h < 0$, the cycles $2[a^-] + [b^-]$ become $2[c^-] + [d^-]$, while the cycles $[b^-]$ transport to $[d^-]$. Moving to the level-sets $\Lambda_{j,h}$ with $j > 0, h > 0$, the cycles $2[c^-] + [d^-]$ become $2[c^+] + [d^+]$, while the cycles $[d^-]$ transport to $[d^+]$. Closing the path and moving back to the base fiber $\Lambda_{j,h}$ with $j < 0$ and $h > 0$, one obtains the final cycles $2[a^+] + [b^+]$ and $[b^+]$.

The conclusion is that there is an index-2 subgroup of the first homology group $\Lambda_{j,h}$ (with $j < 0, h > 0$), generated by $2[a^+]$ and $[b^+]$ that can be parallel transported along the path γ around the essential singularity in $(0, 0)$, through the singular locus $(-\frac{1}{2}, 0) \times 0$. The parallel transport defines a map from this subgroup onto itself that, written with respect to the basis $2[a^+], [b^+]$, is represented by the matrix $\left(\begin{smallmatrix} 1 & 0 \\ 1 & 1 \end{smallmatrix}\right)$. This is what we planned to prove.

5. Examples with monodromy in SL(2, $\mathbb{Z}_{(q)}$). Degenerate hyperbolic singularities

It is natural to extend the system in Section 4 to a q-indexed family of completely integrable systems, with $q \geqslant 2$. Consider the 4-dimensional completely integrable system defined in the phase space $\mathbb{C}_z \times \mathbb{C}_w$ and given by the two commuting functions

$$J = \frac{1}{2}\big(|z|^2 - q|w|^2\big), \qquad H = \sqrt{q}\,\Im(z^q w) + q|z|^q\,|w|^2.$$

These two functions define the momentum map $(J, H) : \mathbb{C}^2 \to \mathbb{R}^2$ that has compact and connected level sets. The image of the momentum map is qualitatively the same as that studied in Section 4. The critical values of the momentum map are of three types: the origin, whose fiber is a *pinched torus*, the set of points $(-\frac{1}{2}, 0) \times \{0\}$, whose fibers are *$q$-curled tori C_q*. The points in the boundary of the momentum domain are uninteresting to us, their fibers are circles.

The same arguments of Section 4 allows the immersion of the level sets $\Lambda_{j,h}$ in $\mathbb{C} \times S^1$. The immersed submanifold can be described precisely in the same way with two differences:

1. When j is in the interval $(-\frac{1}{2}, 0)$ the curves in Fig. 7 left, when rotating, must be lowered q-times the angle of rotation.
2. When j is positive, the curves obtained by sectioning have q hunchbacks (instead of 2) and, rotating, must be lowered by $1/q$ the angle they have been rotated, so that after one turn each hunchback is glued to the one immediately below.

The same analysis as in Section 4 shows that the only surfaces that are not two dimensional tori are those with $h = 0$ and $-\frac{1}{2} < j < 0$, they are generated by rotating the curves that touch the ϑ-axes and are q-curled tori. The fundamental group of a q-curled torus is generated by two cycles α and β that must satisfy the relation $\alpha\beta^q = \beta^q\alpha$. The topology of these singular manifolds can be easily described with cut-and-paste arguments, using the representation in Fig. 5

Consider now a loop γ that winds around the origin once as in Fig. 6 right. As in Section 4, the definition of the cycles $b^{\pm}$ and $d^{\pm}$ follows from the circle action of the $1 : -q$ harmonic oscillator, whose Hamiltonian is J. The cycles $a^{\pm}$ and $c^{\pm}$ are precisely those in Figs. 8 and 9, with the difference in the number of hunchbacks (that are q) in the second set of figures.

With this choice of cycles, one easily sees that a^+ maps to α, while b^+ maps to β^q. On the other side, a^- maps onto $\alpha\beta^{-1}$, while b^- maps to β^q. This is precisely what happens in the semi-local model described in the Introduction. To close the path, we observe that the cycle a^+ transports to the cycle c^+, the cycle b^+ transports to the cycle d^+, the cycle a^- transports to the cycle c^-, and the cycle b^- transports to the cycle d^-.

In homology, the smoothly varying homology cycles $q[a^+]$ parallel transport up to the critical fiber $\Lambda_{j,0}$ to the cycle $q[\alpha]$ while the cycles $[b^+]$ transport to the cycle $q[\beta]$. From the other side, the cycle $q[\alpha]$ is the image of the cycles $q[a^-] + [b^-]$, while the cycle $q[\beta]$ is the image of $[b^-]$. So, the parallel transport deforms the cycles $q[a^+]$ into the cycles $q[a^-] + [b^-]$ and $[b^+]$ to $[b^-]$.

Continuing the parallel transport to the level-sets $\Lambda_{j,h}$ with $j > 0$ and $h < 0$, the cycles $q[a^-] + [b^-]$ become $q[c^-] + [d^-]$, while the cycles $[b^-]$ transport to $[d^-]$. Moving to the level-sets $\Lambda_{j,h}$ with $j > 0, h > 0$, the cycles $q[c^-] + [d^-]$ become $q[c^+] + [d^+]$, while the cycles $[d^-]$ transport to $[d^+]$. Closing the path and moving back to the base fiber $\Lambda_{j,h}$ with $j < 0$ and $h > 0$, one obtains the final cycles $q[a^+] + [b^+]$ and $[b^+]$.

The conclusion is that there is an index-q subgroup of the first homology group $\Lambda_{j,h}$ (with $j < 0, h > 0$), generated by $q[a^+]$ and $[b^+]$ that can be parallel transported along the path γ around the singular value $(0, 0)$, through the singular locus $(-\frac{1}{2}, 0) \times 0$. The parallel transport defines a map from this subgroup onto itself that, written with respect to the basis $q[a^+], [b^+]$, is represented by the matrix $\left(\begin{smallmatrix} 1 & 0 \\ 1 & 1 \end{smallmatrix}\right)$. This proves that the monodromy matrix associated to these systems is $\left(\begin{smallmatrix} 1 & 0 \\ 1/q & 1 \end{smallmatrix}\right)$.

6. Appendix

Here we briefly explain how we obtained the description of the levels $\Lambda_{j,h}$ in Section 4 (and 5). The proof of this last fact is a little cumbersome, it does not help intuition, and it makes use of polar coordinates (see [13]). We write it here for the sake of completeness. All points in $\{0\} \times S^1_{\varphi}$ belong to the level $\Lambda_{j,0}$, so the level sets $\Lambda_{j,h}$ with $h \neq 0$ can be algebraically defined by assuming that $w = se^{i\vartheta}$ with $s \neq 0$. The equations $H = h$ becomes $\sin(2\varphi + \vartheta) = \frac{h}{2\sqrt{2}s(s^2+j)} - \sqrt{2}s = \sigma_{j,h}(s)$ which can be rewritten as

$$\varphi = \frac{1}{2}\big(\arcsin\big(\sigma_{j,h}(s)\big) - \vartheta\big). \tag{1}$$

The function $\sigma_{j,h}(s)$ is strictly decreasing from $+\infty$ to $-\infty$ when h is positive, and goes from $-\infty$ back to $-\infty$ when h is negative, changing only once from increasing to decreasing and reaching a number less than zero at its maximum. The plot of the function $\sigma_{j,h}(s)$ for h positive, zero and negative is shown in Fig. 10.

Also the circle $\{0\} \times S^1_{\vartheta}$ lays in the level set $H = 0$, and hence it does not lay in any other level set. All the other levels $H = h \neq 0$ do not contain $z = 0$. Also in this case, resorting to polar coordinates $z = re^{i\varphi}$, one has that the

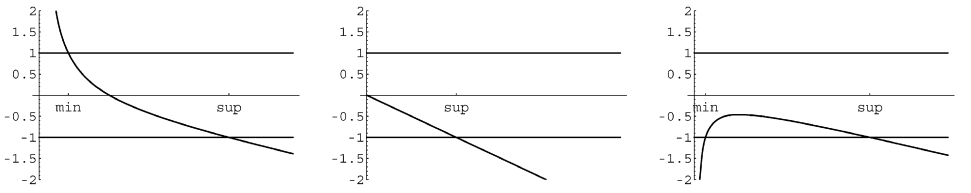

Fig. 10. The qualitative graphs of the functions $\sigma_{j,h}(s)$ and $\rho_{j,h}(r)$ for h positive, zero and negative. The interesting part of the graph is that between -1 and 1.

equation $H = h$ becomes $\sin(\vartheta + 2\varphi) = \frac{h}{r^2\sqrt{r^2-2j}} - \sqrt{r^2 - 2j} = \rho_{j,h}(r)$, that is

$$\vartheta = \arcsin\big(\rho_{j,h}(r)\big) - 2\varphi.$$

The function $\rho_{j,h}$ has a graph that is qualitatively the same as that of $\sigma_{j,h}$.

7. Conclusions

One natural question to ask is whether the degenerate singularities of a system with monodromy in $\mathbb{Z}_{(q)}$ can be slightly perturbed, in the family of completely integrable systems, into non-degenerate singularities. If this perturbation was possible, the consequence would be that fractional monodromy is not preserved under completely integrable perturbations. It is in fact impossible that the composition of matrices in $\mathrm{SL}(2, \mathbb{Z}_{(2)})$ give rise to a matrix with coefficients in $\mathbb{Z}_{(q)}$ with q not a power of 2. There are hence two possibilities

1. The only fractional monodromy which is stable under completely integrable perturbations is that in $\mathbb{Z}_{(2)}$.
2. The classification of singularities of non-degenerate type is not topologically exhaustive.

It is very likely that the second fact is true. Unfortunately, completely integrable perturbations, that is a family of Poisson commuting functions $F_i(p, q, \varepsilon)$ smoothly depending on the real parameter ε is, to our knowledge, not studied in the literature. Easier to describe is a more restrictive kind of perturbation in which the commuting functions are $J_1, \ldots, J_{n-1}, H$ and only H is perturbed. In the case of the functions in Section 5, we cannot find a perturbation of H so to have a completely integrable system with non-degenerate singularities.

Acknowledgements

This work was supported by the EU network HPRN-CT-2000-0113 MASIE—Mechanics and Symmetry in Europe. A first draft of this paper was written during a visit at the MREID of Dunkerque, I thank the Research Center for the hospitality. I also wish to thank Zhilinskiì and Sadovskiì for sharing with me their ideas on fractional monodromy. My arguments in Section 4 and 5 can be reconduced to their (and Nekhoroshev's) idea of defining cycles by intersections with well chosen hyperplanes [11,12]. I also thank R. Cushman, K. Efstathiou, and F. Fassò for enlightening discussions on the subject.

References

[1] A.V. Bolsinov, S.V. Matveev, A.T. Fomenko, Topological classification of integrable Hamiltonian systems with two degrees of freedom. List of systems of small complexity, Russian Mathematical Surveys 45 (2) (1990) 59–94.
[2] R. Cushman, L. Bates, Global Aspects of Classical Integrable Systems, Birkhauser, 1997.
[3] R. Cushman, J.J. Duistermaat, The quantum mechanical spherical pendulum, Bulletin of the AMS (New Series) 19 (1988) 475–479.
[4] R. Cushman, D. Sadovskiì, Monodromy in perturbed Kepler systems: hydrogen atom in crossed fields, Europhysics Letters 47 (1999) 1–7.
[5] B.A. Dubrovin, A.T. Fomenko, S.P. Novikov, Modern Geometry, Methods and Applications Part II. Introduction to Homology Theory, Springer-Verlag, 1985, GTM104.
[6] J.J. Duistermaat, On global action-angle coordinates, Communications on Pure and Applied Mathematics 33 (6) (1980) 687–706.
[7] H. Dullin, A. Giacobbe, R. Cushman, Monodromy in the resonant swing spring, Physica D 190 (1–2) (2004) 15–37.
[8] K. Efstathiou, D.A. Sadovskiì, R.H. Cushman, Fractional monodromy in the $1 : -2$ resonance, Advances in Mathematics 209 (1) (2007) 241–273.
[9] A. Giacobbe, R. Cushman, D. Sadovskiì, B. Zhilinskiì, Monodromy of the quantum 1:1:2 resonant swing spring, Journal of Mathematical Physics 45 (12) (2004) 5076–5100.
[10] V. Guillemin, A. Uribe, Monodromy in the quantum spherical pendulum, Communications in Mathematical Physics 122 (1987) 563–574.
[11] N. Nekhoroshev, D. Sadovskiì, B. Zhilinskiì, Fractional monodromy of resonant classical and quantum oscillators, Comptes Rendus Mathematique 335 (11) (2002) 985–988.
[12] N. Nekhoroshev, D. Sadovskiì, B. Zhilinskiì, Fractional Hamiltonian monodromy, Ann. Henri Poincaré 7 (6) (2006) 1099–1211.
[13] D.A. Sadovskiì, K. Efstathiou, No polar coordinates, in: J. Montaldi, T. Ratiu (Eds.), Geometric Mechanics and Symmetry: the Peyresq Lectures, Cambridge University Press, 2005.
[14] S. Vu Ngoc, Quantum monodromy in completely integrable systems, Communications in Mathematical Physics 203 (1999) 465–479.
[15] H. Waalkens, P.H. Richter, H.R. Dullin, The problem of two fixed centers: bifurcations, actions, monodromy, Physica D 196 (2004) 265–310.
[16] N.T. Zung, Symplectic topology of integrable Hamiltonian systems, I: Arnold–Liouville with singularities, Compositio Mathematica 101 (1996) 179–215. See also Errata at http://picard.ups-tlse.fr/~tienzung/Maths/publications.html.